



## Unsteadyflow simulation of a vertical Axis Wind Turbine:A two-dimensional study with emphasis on CFD turbulence models.

RadkarTushar<sup>a</sup>, Dr.VilasWarudkar<sup>b</sup>

<sup>a</sup>Fellow of Masters in Industrial Design, Maulana Azad National Institute of Technology (MANIT), Bhopal 462003(MP), India.

<sup>b</sup>Assistant Professor, Department of Mechanical Engineering, MANIT, Bhopal 462003 (MP), India.

**Abstract:** In this work we find out suitable settings with which 2D analysis of Darrieus VAWT (Vertical Axis Wind Turbine) can be performed in ANSYS Fluent for acceptable results also this work provides optimum Tip-Speed Ratio for performance optimization. Aerofoil shapes like NACA-0021 & S-1046 were selected for this study. Analysis through various CFD softwares is relatively economical and less time consuming, but results of such software's are greatly influenced by the input parameters like Velocity, Viscosity, Turbulence at input, boundary conditions, etc; also the mathematical models incorporated in these study. Due to input conditions the flow comes out to be fairly turbulent encouraging us to consider Turbulence model widely used in such type of studies, they are k- $\epsilon$ , k- $\omega$  & SST (Shear Stress Transport). The outcomes of these three models were compared for both aero-foil profiles focusing on areas like near blades, in rotor domains, in fluid domains, etc. SST model comes out as best among them in terms of predicting variations in fluid and near wall domains. This study will help future VAWT researchers to set fluent solver for quick and acceptable result. Analysis on 2D aerofoil was performed with these settings and compared with experimental results from literatures to check the orientation of this study. Parametric optimizations of VAWT under different TSR ratio are done.

### 1. Introduction:

VAWT was developed in late 1<sup>st</sup> century but the focus on development was faded due relatively more advantageous HAWT (Horizontal Axis Wind Turbine) developed in early 2<sup>nd</sup> century. In recent decades issues like weight & scale of installations, environmental impacts, remoteness of plants, operational noise, increased problems in transportation of parts, etc paved in shift of research orientation back to VAWTs. VAWTs prima facie looks like solution to above issues. Installing wind turbine on the site where it is needed shows benefits like reduction in transmission losses and cable costs, studies have shown that VAWTs are more suitable in areas like industrial installations, townships (Mertens, 2006; Ferreira et al., 2007a; Stankovic et al., 2009; Mewburn-Crook, 1990), as low rotational speed keeps operational sound level of VAWTs in permissible range also aesthetically they are more suitable, threats to birds with VAWT is less as the solidity of swept area will give visible obstacles and time for birds to maneuver their flight. Offshore installations with HAWT are costly as it requires large floating platforms and multiple supports-connections with sea base to hold them to desired positions, on other hand less moving components, no yawing mechanism, installation of heavy component near base results in lower controlling torque and hence lighter platform making VAWT installations offshore more viable (Willy Tjiu et al., 2015). Out of nearly 314 thousand only around 12 thousand wind turbines are installed offshore amounting 3% of global wind energy production from it (global wind energy council 2015). Omni-directionality without a yaw control; more efficient in turbulent environments such points encourages research on VAWT especially for offshore use.

### 2. Wind Turbine design:

3D model was generated using CATIA as in Figure I; and 2D model was extrapolated from middle section of 3D model. The shaft supporting Darrieus VAWT was part of that extrapolation but for simplicity of special domain shaft was neglected. Smaller dimensions of shaft compared to chord of blades allow neglecting its effect, results of some works agrees to this statement (Rosario Nobile et al., 2014; Kadhim Suffer 2014).

Aim of present work was to finalize the ANSYS Fluent setup for computing flow behavior and various performance parameter of Darrieus VAWT. At different Tips-Speed Ratios output parameters like torque, pressure coefficient, and moment were recorded. Wind speed was taken as 6m/s as over the span of year the average wind velocity comes out to near 6m/s for large number of areas with wind energy potential. The main geometrical features of the tested rotors are summarized in Table 1 & Table 2. Two different profiles with different sizes are selected to see the variations in pressure and velocity contours between two different Reynolds number (Re) as the turbulence models may have sensitivity to Re.



Both profiles selected have their local center of pressure at .367 times chord length from leading tip of profile this can be easily obtained from wireframe module of CATIA.

Table 1. Main geometrical features of the tested model with NACA 0021

| $D_{\text{rotor}}[\text{mm}]$ | $H_{\text{rotor}}[\text{mm}]$ (2D simulation) | $c[\text{mm}]$ | $N[-]$ | $s[-]$ |     |  |  |
|-------------------------------|---|----------------|--------|--------|-----|--|--|
| Blade profile NACA 0021       | 2000  | 2000           | 200    | 3      | 0.6 |  |  |

Table 2. Main geometrical features of the tested model with S1046

| $D_{\text{rotor}}[\text{mm}]$ | $H_{\text{rotor}}[\text{mm}]$ (2D simulation) | $c[\text{mm}]$ | $N[-]$ | $s[-]$ |     |  |  |
|-------------------------------|---|----------------|--------|--------|-----|--|--|
| Blade profile NACA 0021       | 1060  | 2000           | 100    | 3      | 0.6 |  |  |

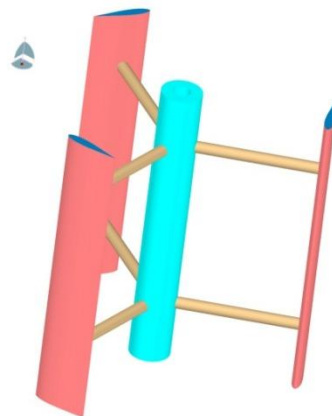


Figure I 3D skewed model of rotor

### 3. Computational setup of Spatial domains:

As the aim of the present numerical investigation was to determine the operation of andarrieus VAWT, the engagement of fixed and rotating domains were required. As shown in Figure II, the 2D fluid domain was composed of three distinct domains: a fixed rectangular outer fluid domain with circular aperture; disk shaped rotating domain to be consider as rotor; and a circular inner fluid domain to fit into the inner aperture. Fixed rectangular outer domain was identified as the wind tunnel domain; the circular inner domain was identified as the fluid domain for the VAWT. Such disk shaped arrangement is for ease in meshing to very fine extent in near blade areas without much increase in number of elements.

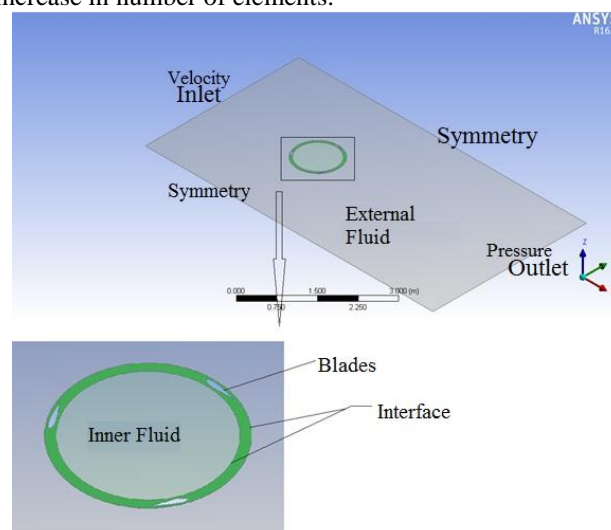


Figure II Spatial Domain



Analysis on S1046 was done with two domain model: outer fluid domain; and inner rotating domain. This was done to check the disturbances in fluid contours with multiple moving interfaces. Meshing was done in ANSYS CFX 16.2

### 3.1. The wind tunnel domain:

Figure II shows the boundary conditions employed in the wind tunnel domain. The wind tunnel domain represents the outside fluid around the rotor. The width of the wind tunnel domain was set to 8 times the rotor diameter. In accordance with Alessandro Bianchini et al., (2015): the inlet boundary condition was set to 5 rotor diameters upwind, as an inlet condition close to the rotor can give incorrect results; the outlet boundary condition was set to 10 rotor diameters downwind, in order to monitor wake formations during the operation of the wind turbine. The inlet boundary condition was defined at the left side of the wind tunnel, with a turbulence intensity of 10% in order to simulate the operation of the wind turbine in the built environment. The outlet boundary condition was defined at the right side of the wind tunnel with a relative pressure of 0 Pa; it represents an open condition. A structured mesh was employed for the fixed rectangular outer domain, with the intention of reducing computational time. Two wall boundary conditions, with free slip wall, were used for the side walls with the purpose of neglecting solid blockage effects, symmetry boundary conditions ensures the viscous forces will not dilute results. An interface boundary condition was employed between the circular hole in the wind tunnel and the rotor (or stator-rotor) domain also in inner hole of rotor and inner fluid domain with sliding mesh technique in order to guarantee fluid continuity and faster result convergence. There are some other techniques to study wind turbine like 6 Degree of Freedom which is used to see actual torque generated due to lift force when turbine is stationary. But as VAWTs in study are unable to start on its own and initial starting torque is needed so the study with sliding mesh technique seems appropriate to use.

### 3.2. The rotor domain & inner fluid domain:

Figure II shows the rotor subdomains with green colour highlight. An angular velocity was imposed to rotor domain this angular velocity was varied for subsequent iterations. The two subdomains were fitted into the circular hole of the wind tunnel domain. The rotor domain was meshed by using unstructured elements, as they can follow complex geometries such as aerofoils. The two distinctive subdomains were created in order to have the freedom to change the mesh quality around the rotor and verify mesh dependency. Interface boundary conditions were used between the two subdomain sides in order to guarantee fluid continuity. For faster convergence, the size of the cells between the interface regions was tried to match. Wall boundary conditions were imposed on the rotor blades.

CFD student version of ANSYS Fluent 16.2 & educational version of ANSYS CFX 14.0 were employed. The numerical solver used is based on solving the Unsteady Reynolds Averaged Navier Stokes (URANS) equations by employing a finite-volume method. A challenge in any CFD code is the selection of the right turbulence model, which is highly dependent on the nature of the flow considered. Its mathematical nature can affect computational resources, time and result accuracy. Wang et al. (2010) show that the most popular turbulence models, adopted in the CFD community, are mainly Direct Numerical Simulation (DNS), Large Eddy Simulation (LES) and RANS. In present study special RANS with 3 different turbulence sub-models were analyzed, they are k- $\epsilon$ , k- $\omega$  & Shear Stress Transport (SST) models.

### 3.3. Mesh dependency study:

Some simulations were carried out to check the extent of deviation in CFD results with varying mesh quality. SST turbulence model was selected. Coarse mesh was unable to trace aerofoil shape properly so it was neglected thoroughly; and the numerical study was run for three different mesh resolutions: medium mesh with elements in range of 3 Lakh, fine mesh with near 13 lakh elements & very fine mesh with nearly 47 lakh. The objective was to select the most appropriate mesh that can guarantee low computational costs and good result accuracy. The case considered in this study was based on a three straight-bladed open rotor with wind speed 6 m/s and tip speed ratio 2. This case was selected because the best performance of the wind turbine was expected to be achieved for a value around this TSR.

There good agreement of results with medium and fine mesh. Solutions of both these mesh resolutions were close to each other. Figure III & Figure IV shows output parameter  $c_d$  for medium and fine mesh both shows similar trend with closer values. Flow Time of Figure III & Figure IV should be considered while comparing both as earlier one was computed for more than two rotations and next one was for single rotation. When the setup was run with very fine mesh the results were contradictory, there were fluctuations in residuals and after as much as 150 iterations in single time step convergence was not achieved. Moving further the residuals started diverging so the computation was stopped Figure V shows the diverging trend.

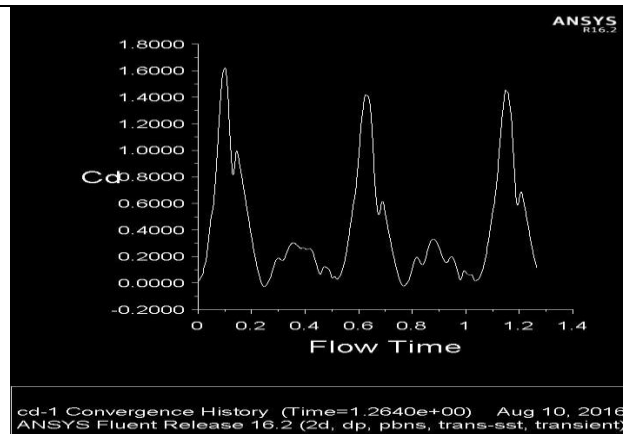


Figure III Coeff. of Drag with Medium mesh

Convergence is criteria where the results of successive iterations show very small deviations in the range of (0.0001) and in divergence gap between values increases. It is clear that the simulation time is highly dependent on the number of elements considered. It appears that the medium mesh is a good compromise in terms of computational costs. Consequently, the following mesh was employed for all the successive simulations considered in this study. Time steps were taken .0015sec to cover one degree rotation in each rotation.

Table 3 Number of elements and simulation time for the three meshes analysed.

| Mesh resolution    | Medium mesh | Fine mesh | Very fine mesh |
|--------------------|-------------|-----------|----------------|
| Number of elements | 300,000     | 1300,000  | 4700,000       |
| Simulation time    | 8 hrs       | 17hrs     | 5 hrs          |

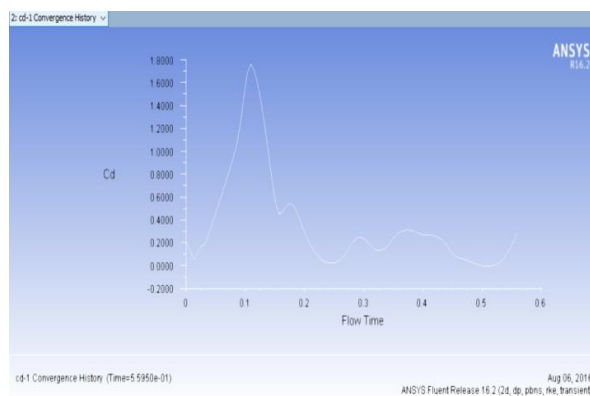


Figure III Coeff. of Drag with Fine mesh

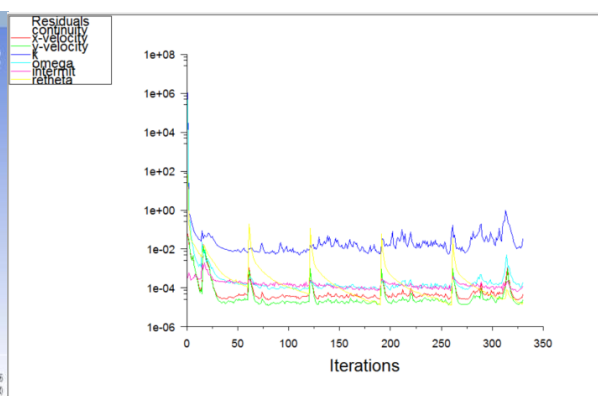


Figure V Residuals of very fine mesh size

### 3.4. Turbulence model study:

In this numerical analysis, three different URANS turbulence models were considered: standard  $k-\epsilon$  model, standard  $k-\omega$  model and SST model. In this case a medium mesh and a time step of 0.0015s were selected in accordance to the previous sections. The outcomes of these models are discussed in result sections.



### 3.5. CFD Validation:

In this section, an experimental data was compared with the numerical simulations of the NACA-0021 profile and S1046 was not focused for obvious reason of turbulence model, setup and mesh quality. The scope was to verify the accuracy of CFD data with experimental data. Lift and drag coefficients were obtained running simulations at different angle of attacks. The experimental data is available on NACA server.

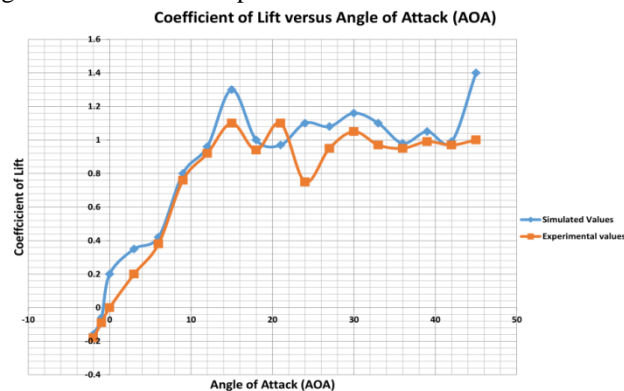


Figure IV Coefficient of lift vs Angle of Attack

With some trend deviation, roughly both plots follow similar trends. As in Figure V & Figure VI Simulated data are with higher values compared to experimental data, which could be associated with the effect of finite blade length and spoke drag (tip drag at blade ends) that was not considered in the 2D numerical analysis. Difference in data is with near 15% with exceptions in couple of places where error touched to 30%. This simulation is done with the nodes size which in harmony to the primary computation of 3 Bladed Darrieus VAWT in 2D. This way of validation is faster than validating with experimental work of whole VAWT; without affecting accuracy as the torque coefficient which would generally be compared in (Rosario Nobile et al., 2014) are outcome of lift and drag coefficient only.

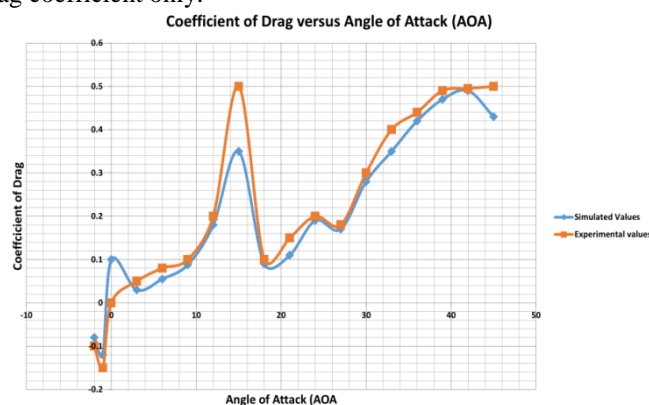


Figure V coefficient of Drag vs Angle of Attack

### 3.6. Parametric optimization:

Further study was done on SST model to see the output parameters like power coefficient and torque coefficient which in turn give torque. Here TSR is taken in between .2 to 2.2 in five equal intervals. Here to enlarge the span of research, inlet velocities as well as angular velocity of rotation is also changed. There can be many combinations of wind velocity and angular velocity but common combination was selected.

## 4. Results:

The CFD code was able to visualize the basic physics behind a VAWT, and it can be used as an alternative to wind tunnel tests.

### 4.1. k-ε turbulence model

Figure VI & Figure VII shows computational result of S1046 blade profile with TSR 2, inlet velocity 6m/s and so on of 301<sup>0th</sup> rotation; velocity & pressure contours, velocity & pressure trails & the turbulence in downstream is clearly visible in fluid domain. But near Blade walls changes are not properly predicted, this is in



acceptance with literatures as **k-  $\epsilon$  model** is less efficient in near wall simulations. Lower values of the torque coefficient & other output parameters also support this statement. The results with NACA 0021 are of similar nature. This model needs more time to achieve steady conditions which can be seen from Figure XII & Figure XIII, computation needs to be run for larger no of rotation for this. But the time taken for each time step is less than other models. Every iteration took about 1min with 50 iteration per time steps.

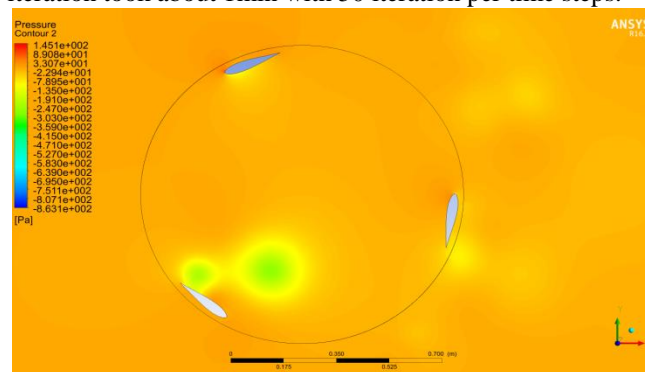


Figure VI pressure contours of k-  $\epsilon$  model

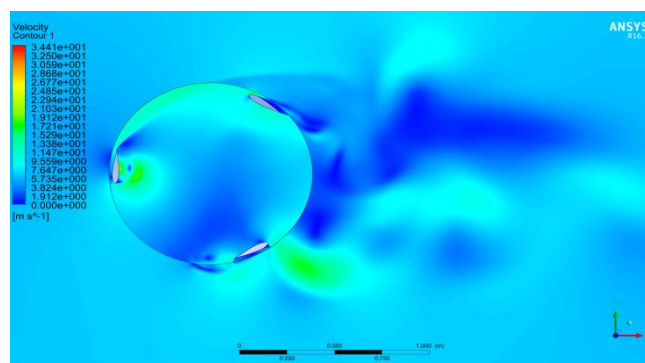


Figure VII Velocity contours of k- $\epsilon$  model

#### 4.2. k- $\omega$ turbulence model:

Figure IX & Figure X shows computational result of S1046 blade profile with TSR 2, inlet velocity 6m/s and so on of 301<sup>th</sup> rotation; in form of velocity & pressure contours. Here near Blade walls changes are well predicted as in literatures as **k-  $\omega$  model** gives better results in near wall simulations. Better values of the torque coefficient & other output parameters which are in vicinity to blade but in fluid domain the contours are weak. The results with NACA 0021 are of similar nature. This model needed lesser time to achieve steady conditions which can be seen from Figure XII & Figure XIII, computation needs to be run for small no of rotation for this.

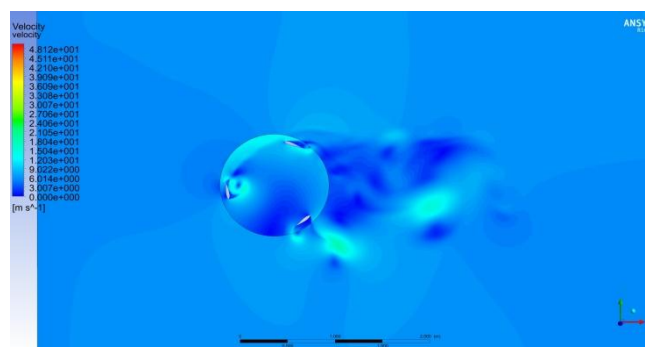


Figure VIII velocity contours of k-  $\omega$  model



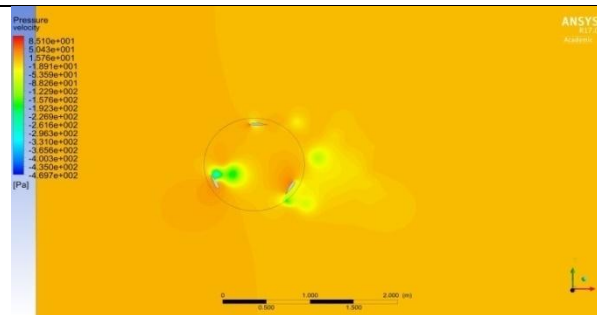


Figure IX Pressure contours of k- $\omega$  model

#### 4.3. SST turbulence model:

SST model is the combination of two different turbulence models: the k- $\omega$  model in the inner parts of the boundary layer, and the k- $\epsilon$  model in the free-stream. Pressure and velocity contours are seen in single diagram in Figure XI, the contours are properly visible near blade and fluid domain. This model needs higher processing power each iteration of this model consumes 30mins. Computation achieve steadiness in second quarter of rotation.

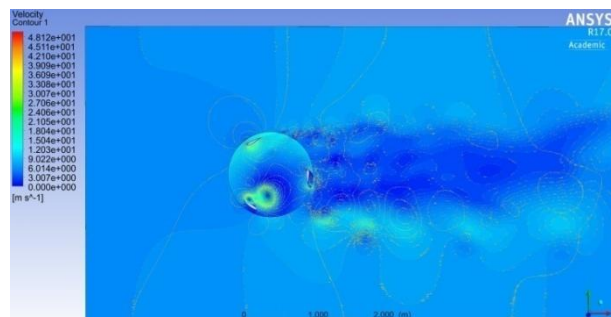


Figure X combined pressure & velocity contours of SST model

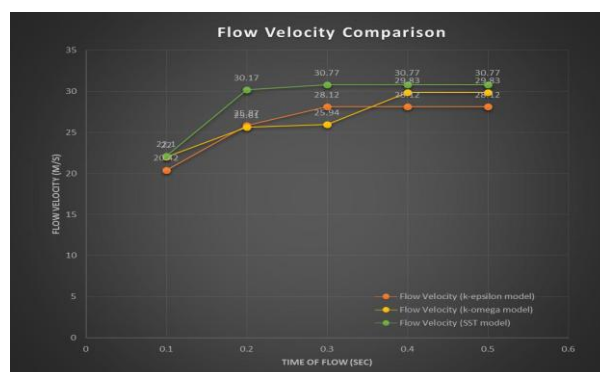


Figure XI Flow Velocity in different model

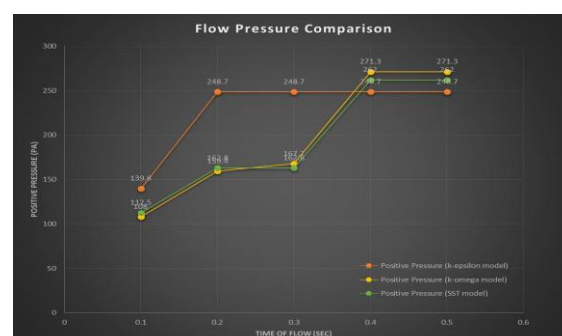


Figure XII Flow pressure for all models



Figure XII shows extent of velocities at different points in computational space for all three models at different time (which also shows angular displacement of rotor). It is clear from fig that SST model achieves steadiness earliest among three and k- $\epsilon$  took more time than other two.

Figure XIII shows pressure variation in k- $\epsilon$  model achieves steadiness very early this is may be due to in sensitivity to wall changes while other two models shows closeness in result.

Figure XIII shows the cyclic nature of  $c_m$  which is aggregate of  $c_m$  all three blades. These contours are periodic after every  $120^\circ$  of rotation as blades are placed with  $120^\circ$  between them.

#### 4.4. Parametric optimization:

Figure XV shows torque on rotor are maximum at TSR 1 where wind velocity was 8m/s, it should be noted that here wind velocity of 12m/s was also considered but due to lower Torque Coefficient final torque was low.

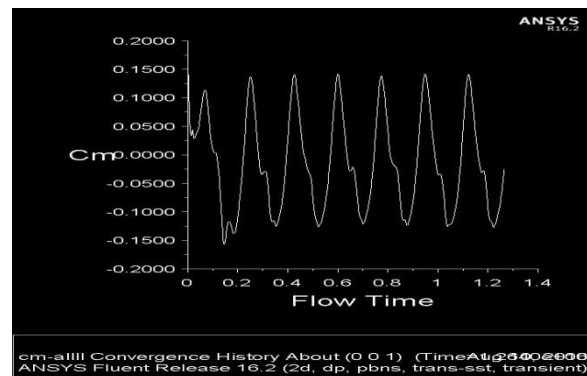


Figure XIII coefficient of momentum in SST model

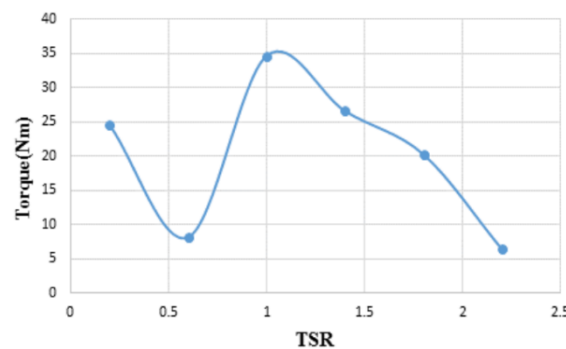


Figure XIV torque to TSR plot

Figure XVI shows maximum power coefficient at TSR 1.8 which is closer to assumption of higher power at TSR 2.

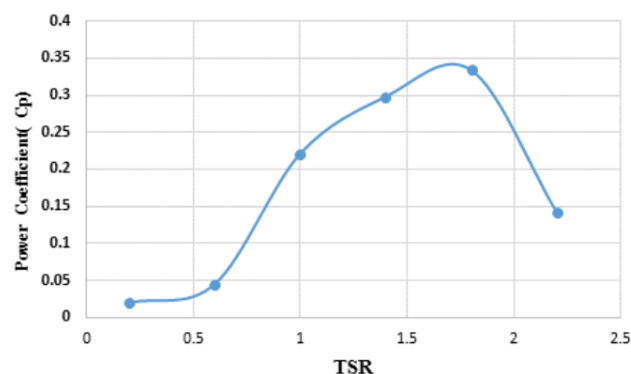


Figure XV Coefficient of Power to TSR





## 5. Conclusion :

In this paper the performance of Darrieus straight-bladed VAWT has been presented. In the first part of the paper, VAWT was examined in order to select a reasonable mesh resolution, time step to be implemented in the successive CFD simulations. A CFD validation of the airofoil was also conducted. In the second part of the paper, three different cases of turbulence model were examined in presenting pressure and velocity range at different time steps.

Paper has shown the simulation time is affected by mesh resolution. It is evident that too much fine meshing would result in drastic increase in simulation time and the divergence in solution. Turbulence models also affect the results as models have their specific location where it can give accurate results. Among three models SST is proved to be accurate near wall and in fluid domain on the cost of higher processing power and time. Plots of  $c_d$  &  $c_m$  are in acceptable ranges. Different approach of studying few out of many combinations showed that higher wind velocities does not always produce high torque or power coefficient.

## Acknowledgements:

Simulations of this work in video form can be seen in following links:

- [https://youtu.be/1cKHla-7\\_6Q](https://youtu.be/1cKHla-7_6Q),
- <https://youtu.be/l-0cuxZtCKc>,
- <https://youtu.be/eiXWR09MyXI>,
- <https://youtu.be/QYZ19cWKeas>, etc

## References:

- [1]. Willy Tjiu, TjukupMarnoto, Sohif Mat, MohdHafidzRuslan, KamaruzzamanSopian. Darrieus “vertical axis wind turbine for power generation I: Assessment of Darrieus VAWT configuration”. Renewable Energy 75(2015) 50-67.
- [2]. Rosario Nobile, Maria Vahdati, Janet F. Barlow, Anthony Mewburn-Crook, “Unsteadyflow simulation of a vertical axis augmented wind turbine: A two-dimensional study”. J. Wind Eng. Ind. Aerodyn. 125 (2014) 168–179
- [3]. Bravo, R., S. Tullis, and S. Ziada. "Performance testing of a small vertical-axis wind turbine", Proceedings of the 21st Canadian Congress of Applied Mechanics (CANCAM07), Toronto, Canada, June. 2007.
- [4]. Paraschivoiu, I., O. Trifu, and F. Saeed. "H-Darrieus wind turbine with blade pitch control", International Journal of Rotating Machinery 2009 (2009).
- [5]. Tchakoua, Pierre, et al., "A New Approach for ModelingDarrieus-Type Vertical Axis Wind Turbine Rotors Using Electrical Equivalent Circuit Analogy: Basis of Theoretical Formulations and Model Development”, Energies 8.10 (2015): 10684-10717.
- [6]. Lanzafame, Rosario, Stefano Mauro, and Michele Messina, "2D CFD modeling of H-Darrieus wind turbines using a transition turbulence model", Energy Procedia 45 (2014): 131-140.
- [7]. Nobile, R., et al., "Unsteady flow simulation of a vertical axis wind turbine: a twodimensional study", EngD Conference, 2nd July. 2013.
- [8]. Ferreira, CJ Simao, et al., "Simulating dynamic stall in a 2D VAWT: modeling strategy, verification and validation with particle image velocimetry data", Journal of physics: conference series. Vol. 75.No. 1.IOP Publishing, 2007.
- [9]. Chris Kaminsky, Austin Filush, Paul Kasprzak and WaelMokhtar. "A CFD Study of Wind Turbine Aerodynamics", Conference, a CFD study of wind turbine aerodynamics, Ohio, USA. American Society for Engineering Education. 2012.
- [10]. Maleal, Ion, and Horia, "Numerical Simulation Of Vawt Flow Using Fluent". U.P.B. Sci. Bull., Series D, Vol. 76, Iss. 1, 2014
- [11]. V. Beran, M. Sedláček, F. Maršůtk. “A new bladeless hydraulicturbine”. Applied-Energy, Volume 104, April 2013, Pages 978-983.
- [12]. Alessandro Bianchini, Giovanni Ferrara, Lorenzo Ferrari. “Pitch Optimization In Small size Darrieus Wind Turbine”. Energy Procedia 81(2015) 122-132
- [13]. Mertens, S., 2006. Wind energy in the built environment: concentrator effects of buildings (TU Delft)
- [14]. Ferreira, C.J., van Bussel, G., van Kuik, G., 2007a. “2D CFD simulation of dynamic stall on a vertical axis wind turbine: verification and validation with PIV measurements.” Proceedings of the 45th AIAA Aerospace Sciences Meeting and Exhibit, American Institute of Aeronautics and Astronautics, pp. 1–11
- [15]. Stankovic, S., Campbell, N., Harries, A., 2009. Urban Wind Energy
- [16]. Mewburn-Crook, A., 1990. The Design and development of an augmented vertical wind turbine